

## A LOW VOLTAGE-ACTIVATED CALCIUM CONDUCTANCE IN EMBRYONIC CHICK SENSORY NEURONS

E. CARBONE AND H. D. LUX

*Department of Neurophysiology, Max-Planck-Institute for Psychiatry, D-8033 Planegg-Martinsried,  
Federal Republic of Germany*

**ABSTRACT** Isolated Ca currents in cultured dorsal root ganglion (DRG) cells were studied using the patch clamp technique. The currents persisted in the presence of 30  $\mu\text{M}$  tetrodotoxin (TTX) or when external Na was replaced by choline. They were fully blocked by millimolar additions of  $\text{Cd}^{2+}$  and  $\text{Ni}^{2+}$  to the bath. Two components of an inward-going Ca current were observed. In 5 mM external Ca, a current of small amplitude, turned on already during steps changes to  $-60$  mV membrane potential, leveled off at  $-30$  mV to a value of  $\sim 0.2$  nA. A second, larger current component, which resembled the previously described Ca current in other cells, appeared at more positive voltages ( $-20$  to  $-10$  mV) and had a maximum  $\sim 0$  mV. The current component activated at the more negative membrane potentials showed the stronger dependence on external Ca. The presence of a time- and a voltage-dependent activation was indicated by the current's sigmoidal rise, which became faster with increased depolarization. Its tail currents were generally slower than those associated with the Ca currents of larger amplitude. From  $-60$  mV holding potential, the maximum obtainable amplitude of the low depolarization-activated current was only one-tenth of that achieved from a holding potential of  $-90$  mV. Voltage-dependent inactivation of this current component was fast compared with that of the other component. The properties of this low voltage-activated and fully inactivating Ca current suggest it is the same as the inward current that has been postulated in several central neurons (Llinas, R., and Y. Yarom, 1981, *J. Physiol. (Lond.)*, 315:569–584), which produce depolarizing potential waves and burst-firing only when membrane hyperpolarization precedes.

### INTRODUCTION

The Ca conductance of the membrane determines the excitation process in a variety of cells (for review, see reference 1). It is brought about by the opening of electrically operated Ca-selective channels, which have similar kinetic properties in different membranes (2, 3). The Ca system is thought to be kinetically different from the Na system, as substantiated by results from both whole-cell and single-channel currents that have been observed in the same type of cell (4; see also reference 1). However, observations on perfused mammalian ganglionic cells suggest slow Na channels exist (5) that have ensemble properties similar to those of the Ca channels known so far. On the other hand, there is evidence that there is a pacemaking inward Ca current in mammalian central neurons that can be activated even by small depolarizations, but only if a high resting potential or a preceding membrane hyperpolarization is provided (6). This behavior agrees more with that expected from a slow Na system, and many of the described features are difficult to reconcile with results from hitherto studied examples of the Ca conductance.

We report here that in cultured dorsal root ganglion cells, besides the main Ca conductance described previously (7), another voltage-dependent Ca conductance exists that is activated at quite negative membrane potentials and is fully inactivated under the usual resting membrane potential conditions. The voltage sensitivity and the amount of current carried by this system should qualify it to act as a pacemaking device under the previously defined conditions (6).

### MATERIALS AND METHODS

The experiments were performed on dissociated cell cultures of embryonic sensory neurons of *Gallus domesticus*. Cells of the dorsal root ganglia were dissociated (8) from 9–11-d-old embryos and used after incubation of at least 24 h. Cells and recording probes were viewed through a Zeiss (Carl Zeiss, Inc., Ober Kochen, Federal Republic of Germany) inverted microscope with a 32 $\times$  objective. Whole-cell clamp currents were measured according to the method of Hamill et al., 1981 (9). The pipettes were made from Duran glass (Schott Ruhrglas, Mainz, Federal Republic of Germany) and had resistances between 2 and 3 M $\Omega$  when filled with the solution of Table I. Pipette connection and current-voltage (I-V) conversion were as described before (10), except for a 1-G $\Omega$  feedback resistor. Current records were stored on an FM tape recorder at

TABLE I  
COMPOSITION OF SOLUTIONS

Abbreviation	External solutions							pH <sub>o</sub>
	NaCl	CaCl <sub>2</sub>	MgCl <sub>2</sub>	BaCl <sub>2</sub>	Chol-Cl	glucose	Na-HEPES	
	<i>mM</i>							
5Ca	120	5	2	—	—	20	10	7.3
1Ca	120	1	6	—	—	20	10	7.3
30Ca	—	30	2	—	—	185	10	7.3
12OChol	—	5	2	—	120	20	10	7.3
95Ba	—	—	—	95	—	—	10	7.3
	<i>mM</i>							
	CsCl	TEACl	CaCl <sub>2</sub>	EGTA-OH	glucose	Na-HEPES	pH <sub>i</sub>	
	<i>mM</i>							
130Cs	130	20	0.25	5	10	10	7.3	

5 kHz bandwidth. The data were digitized by using either a PDP 11/34 minicomputer (Digital Equipment Corp., Marlboro, Mass) or a digital oscilloscope at rates of 50–200  $\mu$ s. Data were stored on floppy disks and plotted on an XY recorder. During recordings, leakage and capacitive current components were compensated for as much as possible by analogue circuitry. The final compensation was done on digital records using inverted pulse paradigms. The series (electrode) resistance was not compensated. This introduces errors in the limits of 0.1–5 mV in the

potential control of recorded membrane currents of 0.1–1.5 nA and slows the voltage-clamp response (11) so that the maximum response time constants obtained were between 100 and 300  $\mu$ s.

At rest, cells were held at a potential of  $-80$  mV ( $E_h$ ). Before recordings, cell fluids were allowed to equilibrate with the pipette solution by waiting several minutes and observing constant effects of voltage pulses. Test depolarizations to various levels ( $E_t$ ) lasted 70–150 ms and were applied at intervals of 5–15 s. Fast inactivation of Ca currents was determined by the two-pulses procedure (12). The conditioning prepulses lasted 150 ms and varied from  $-100$  to  $-50$  mV. The test potentials were  $-40$  and  $-30$  mV. Effects of the holding potential (ultraslow inactivation; 13, 14) were studied by maintaining the cells for 90 s at various potentials between  $-110$  and  $-60$  mV before the test pulses.

The composition of the solutions used are listed in Table I. All experiments were done in the presence of 3 or 30  $\mu$ M TTX in the external bath. To avoid tail currents carried by K ions, all the external solutions were made K-free. To improve the patch conditions, the osmolarity of the pipette-filling solution was chosen to be 20% lower than that of the cell medium (9). The bath temperature was held at  $12 \pm 0.3^\circ\text{C}$  with a Peltier device and a thermistor in feedback configuration.

## RESULTS

Fig. 1, *a* and *b*, shows a series of current recordings obtained during whole-cell clamp steps to various membrane potentials starting from a holding potential of  $-80$  mV. 3  $\mu$ M TTX was added to the 5 mM Ca bath solution (Table I) in order to block inward Na currents. A slowly

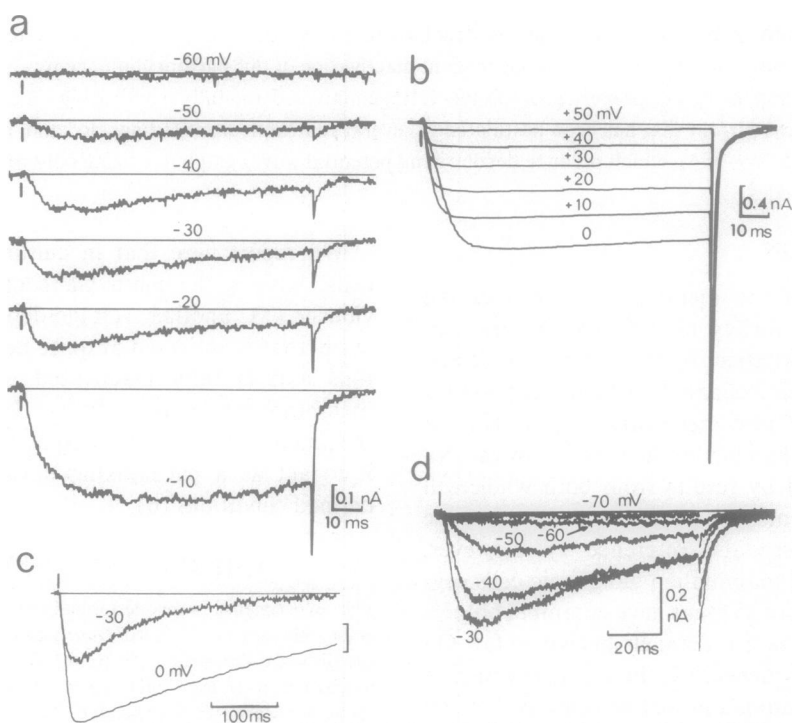


FIGURE 1 Whole-cell clamp currents in 5 mM Ca. (*a* and *b*) Time course of inward Ca currents recorded from the same cell at the membrane potential indicated. Note the reduced amplification and the faster tail currents in part *b*. Out, 5 Ca + 3  $\mu$ M TTX; In, 130 Cs (Table I). (*c*) Time course of inward Ca currents during longlasting depolarizations (400 ms). The conditions are the same as in *a* and *b*, but the cell is different. Note the nearly complete inactivation to a relatively low membrane potential ( $-30$  mV) during the pulse and the slower inactivation time course with stronger depolarization (to 0 mV). The holding potential is  $-80$  mV. Vertical bar, 0.06 nA and 0.2 nA for the records at  $-30$  mV and 0 mV, respectively. (*d*) Inward currents in isotonic Ba recorded at low membrane potentials ( $-70$  to  $-30$  mV, potentials assigned to recordings). The holding and repolarization potential is  $-90$  mV. Out, 95 Ba + 3  $\mu$ M TTX (Table I).

rising inward current appeared at a membrane potential of  $-60$  mV. Its amplitude increased from  $-60$  to  $-40$  mV, and settled between  $-40$  and  $-20$  mV. The inward currents assumed earlier peaks during the clamp steps if the potential levels were increased from  $-50$  to  $-20$  mV. The decay from peak was similarly accelerated and the currents were nearly inactivated (to  $<5\%$  of peak amplitudes) after 400 ms (Fig. 1 *c*). Beyond membrane potentials of  $-20$  mV, the inward currents revealed a second steeper increase, and the I-V relationship resembled that of Ca currents recorded in other dialyzed cell preparations (4, 15–18). Inactivation at potentials more positive than  $-10$  mV was weaker and slower.

Time-to-peak measurements assumed a relative minimum of 12 ms between  $-20$  and  $-30$  mV and a relative maximum of 28 ms at  $\sim 0$  mV, which continuously decreased at positive membrane potentials. To reduce the influence of inactivation on measurements of activation times, the initial portion of the current rise (to half-maximum) was separately investigated. This was done by fitting the sum of two exponentials to the sigmoidal slope of current averages at  $-30$  and  $0$  mV (Fig. 2 *e*). The five parameters of the fitting function, coefficients, exponents, and current level were determined by a least square criterion (10, 19). The so-calculated maximum rates of rise, as well as the half-activation times, showed the same

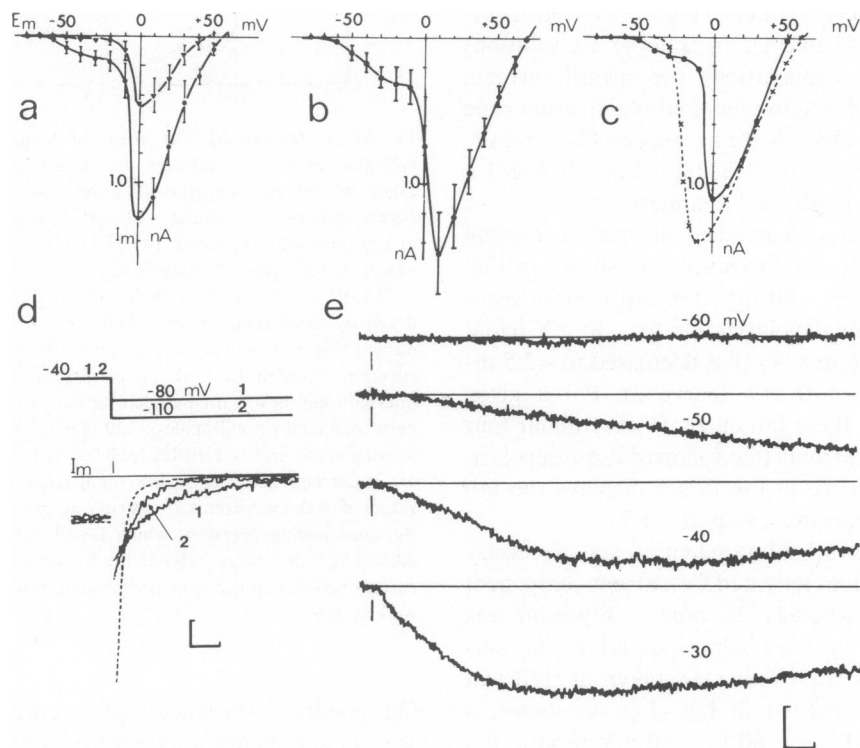


FIGURE 2 (a) Average peak current from five cells plotted against membrane potentials ( $E_m$ ) in the presence of 5 mM (dots) and 1 mM (triangles) external Ca. Bars represent standard deviation from the mean ( $\pm$ SD). The reversal of currents is  $+56$  mV in 5 mM Ca and  $+48$  mV in 1 mM Ca. Both these values are smaller than theoretically expected. As discussed elsewhere (4, 17), this might be a result of a partial Cs permeability of the channel. Assuming there is an identical reversal for the currents activated at low and high voltages, the potential variation required to produce an  $e$ -fold change of the Ca conductance is estimated to be  $\sim 15$  mV at  $-50$  mV membrane potential, whereas it is 5 mV at  $-10$  mV. The holding potential is  $-80$  mV. Out, 5 Ca or 1 Ca +  $3 \mu\text{M}$  TTX (Table I). (b) Plot of averaged peak Ca currents from four cells ( $\pm$ SD) against membrane potential in the presence of 30 mM Ca. Note the increased average values of peak current at low and high voltages. Current reversal is at  $+69$  mV. The maximum peak current, as well as the reversal of current, is shifted by  $\sim +12$  mV. This shift could result from screening of charges at the external membrane surface by the increase in the divalent cation concentration. The holding potential is  $-80$  mV. Out, 30 Ca +  $3 \mu\text{M}$  TTX (Table I). (c) I-V characteristic of peak Ca currents in the presence of 5 mM Ca and 120 mM choline in the bath (Table I, continuous curve). The data are compared with the I-V characteristic of peak Na currents (dashed curve) taken from the same preparation (see Discussion). The holding potential is  $-80$  mV. Out, 120 choline +  $3 \mu\text{M}$  TTX (Table I). (d) Ca tail currents in 5 mM Ca. Traces 1 and 2 were recorded on repolarization to  $-80$  and  $-110$  mV from the peaks of Ca currents during membrane depolarization to  $-40$  mV. The pulse protocol is on top. The dashed curve was recorded under the conditions of the experiments in Fig. 1 *b* with a depolarizing step to 0 mV and repolarization to  $-80$  mV. The holding potential is  $-80$  mV. Vertical bar, 0.5 nA for the dashed curve and 0.5 nA for curves 1 and 2. Horizontal bar, 2.5 ms. The time constants of the tail currents ( $\tau_t$ ) were calculated from fitting an exponential function to the tail recordings, omitting the initial 0.3 ms and the last 20% of the decline. The  $\tau_t$ 's are 5 ms (curve 1), 2.3 ms (curve 2), and 0.8 ms (dashed curve). Out, 5 Ca +  $3 \mu\text{M}$  TTX (Table I). (e) Activation time course of Ca currents recorded on an expanded time scale. The membrane depolarizations are indicated on top of each record. Out, 30 mM Ca +  $3 \mu\text{M}$  TTX (Table I). Bars indicate the onset of depolarizing voltage steps. The time-to-peak at  $-40$  and  $-30$  mV are nearly twice those of Fig. 1 *a*. This is probably owing to a shift of the activation parameters toward more positive voltages with increased external  $\text{Ca}^{2+}$  (30 mM). Bars, 0.1 nA, 5 ms. The holding potential is  $-80$  mV.

intermediate change (by a factor of  $\sim 2$ ) as was seen in the time-to-peak measurements. The results confirm that the rise of the inward current depends on voltage in a nonmonotonic manner.

The currents disappeared entirely with the addition of 1 mM CdCl<sub>2</sub> or 5 mM NiCl<sub>2</sub> to the bath solution. When the bath Ca concentration was reduced from 5 to 1 mM the peak current amplitude decreased as is shown in Fig. 2 *a*. Increasing the extracellular Ca concentration to 30 mM had the opposite effect (Fig. 2 *b*). Note that the currents that appeared below  $-20$  mV were more strongly affected by the reduction of external Ca than the currents activated with stronger depolarizing steps. The same I-V relationship and average amplitudes of currents were obtained if Na in the bath was largely reduced (Fig. 2 *c*) by substituting 120 mM choline (Table I). In isotonic Ba solutions (95Ba; see Table I for explanation), the inward currents (Fig. 1 *d*) showed similar activation and inactivation time courses, but they were about twice as large as Ca currents. All this suggests that currents of the type shown in Fig. 1 *a* flow predominantly through Ca<sup>2+</sup> channels.

Time courses of tail currents sped up with increasing negativity of membrane repolarization. As shown in Fig. 2 *d*, on repolarization to  $-80$  mV, the tail current associated with a membrane depolarization to  $-40$  mV had a time constant of 5 ms (curve 1) that decreased to  $\sim 2.5$  ms on repolarization to  $-110$  mV (curve 2). For a given repolarizing potential, these tail currents were about four times slower than tail currents that followed large depolarizations. The dashed curve in the figure displays the tail current at  $-80$  mV following a step to 0 mV.

A sufficiently negative holding potential was necessary for the low depolarization-activated Ca current component to appear (Fig. 3 *a*), whereas the other component was little affected by varying the holding potential. The normalized peak currents from four cells taken at different holding potentials are plotted in Fig. 3 *b*. As shown, a change in the holding from  $-60$  to  $-90$  mV produced a nearly 10-fold increase in the current amplitude that was measured at  $-40$  mV. The potential of half inactivation was  $-80$  mV. This value is 20 mV more negative than that found under comparable conditions for the ultraslow inactivation of the Na conductance in squid axons (13) and frog nodes (14), as well as in DRG cells (dashed curve in Fig. 3 *b*). However, the steepness of the inactivation-voltage curve of the low voltage-activated current is similar to that of the Na current in this preparation. This was also true for the fast inactivation curve measured with short-lasting (150 ms) conditioning prepulses (Fig. 3 *c*).

## DISCUSSION

Activation-voltage relationships of individual ionic conductances, including previously observed Ca conductances, all show a monotonic change with voltage that is within the range of the presently investigated membrane potentials.

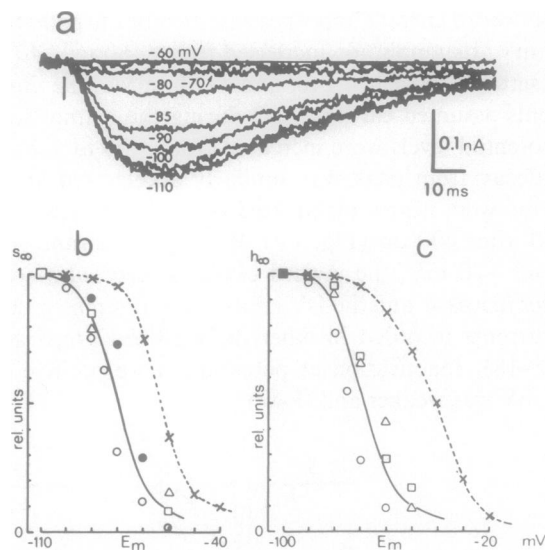


FIGURE 3 (*a* and *b*) The effect of holding potentials on the low voltage-activated Ca currents. (*a*) Superimposed Ca current records taken during step depolarization to  $-40$  mV from varied holding potentials between  $-60$  and  $-110$  mV. The cell was maintained for 90 s at the potentials indicated. (*b*) Normalized peak Ca currents plotted against holding potential (continuous curve). The depolarizations were to  $-40$  mV: The different symbols indicate different cells. The curve was drawn by visual approximation. Out, 5 Ca + 30  $\mu$ M TTX (Table I). The dashed line and crosses refer to the effect of holding on transient Na currents recorded from the same preparation (see text). The same internal solution was used as that for Ca current measurements, but the bath contained (in millimoles): 120 NaCl, 3 KCl, 2 CaCl<sub>2</sub>, 2 MgCl<sub>2</sub>, 20 moles glucose, and 10 HEPES (pH 7.3). (*c*) The fast inactivation process of Ca currents activated at low voltages (continuous line). Normalized values of peak Ca currents at  $-40$  mV are plotted vs. the potential level of the conditioning prepulse, which lasted 150 ms (see Methods). The dashed line and crosses refer to the  $h_{\infty}$  curve of the fast-inactivating Na current taken from the same preparation. Internal and external solutions were as in *b*).

Our results on the whole cell Ca currents of the vertebrate sensory neuron deviate from this empirical feature because they showed an intermediate extremum of activation times, as well as of inactivation times. This discrepancy is resolved if two distinct Ca conductances are assumed to exist. One component compares well with previously described Ca conductances (1, 4, 15–18) in showing (*a*) a strong increase over a relatively small region of voltage ( $-20$ – $0$  mV), (*b*) a fast turn-off on repolarization with time constants well below 1 ms, and (*c*) a weak inactivation with time constants (at 12°C) in the range of seconds.

The newly described type of a Ca conductance was activated at membrane potentials that are  $\sim 30$ – $40$  mV more negative than those of the former. It shows (*a*) a comparably weak voltage dependence, (*b*) a five times slower turn-off at comparable membrane potentials, and (*c*) a complete voltage-dependent inactivation that is much faster than that of the former type of Ca conductance. The inactivation behavior of this low voltage-activated Ca channel resembles in many aspects that of the Na channel

in this and other cultured cell preparations (4, 20, 21), except there is a 20-mV difference in the location of the inactivation-voltage curves. However, the activation properties of this channel are quite different from those of the Na channel in this preparation, which show a steeper voltage dependence of activation (Fig. 2 b) and activation time courses that are at least five times faster at comparable membrane potentials (Carbone, E., and H. D. Lux, unpublished observations).

Interestingly, a TTX-resistant Na conductance was found in rat dorsal root ganglionic cells that is abolished by nominal Ca channel blockers (5). Its voltage dependency and kinetic properties resemble those of the low depolarization-activated Ca conductance of our preparation. However, our results with reduced extracellular Na exclude the possibility that the eventually corresponding Ca channel in chick dorsal root ganglionic cell is permeable to Na ions to a larger extent. It may thus be that the ionic specificity of this avian Ca channel differs from that of mammals.

The existence of a low voltage-activated Ca conductance has already been inferred from the particular features of a Ca-dependent depolarizing response to injected current in inferior olivary neurons of guinea pigs (6). This response appeared to be regenerative and was seen to inactivate at resting potential (of  $-65$  mV) and to 'de-inactivate' in a time-dependent manner with hyperpolarizations of 10 to 20 mV (6). It was concluded that a completely inactivating Ca-dependent depolarizing response initiated burst-like cell firing of thalamic neurons (22) after membrane hyperpolarization. A low voltage-activated and fully inactivating Ca conductance has already been described in the egg cell membrane of a starfish (23). This current was markedly dependent on external sodium but its activation time course could not be clearly separated from that of the more slowly inactivating Ca current.

The presence of a low potential-activated Ca conductance in this and other preparations could eventually be overlooked because of the cell's relatively low levels of holding or resting potentials (7). However, we failed to record this current in several cells from samples of aged cultures 7–10 d), despite the precaution of having high negative holding potentials (see also reference 24). It was also noted in studies on molluscan neurons that increasingly negative holding potentials have little if any effect on Ca activation (10, 25). Thus, it appears that the low depolarization-activated Ca conductance is not ubiquitous in nerve cells.

This Ca conductance was found to be more sensitive to reductions of extracellular Ca, but attempts to separate it pharmacologically have failed so far. Instead, corroborating evidence for this low depolarization-activated and rapidly inactivating Ca conductance comes from single channel observations in isolated (outside-out; 9) membrane patches of the same preparation (26, 27). The channel differs from the hitherto described Ca channel (2, 3, 10) because it activated at quite negative membrane potentials

( $-60$  to  $-40$  mV) and it inactivated quickly and completely as concluded from observations on opening probabilities. Average lifetimes at comparable membrane potentials were about four times longer than those of the previously described Ca channel, whereas single channel currents were somewhat larger (27).

We thank Mrs. I. Kiss and Mrs. H. Tyrlas for perfect technical assistance.

This work was supported in part by a grant from the Deutsche Forschungsgemeinschaft (SFB 220/1A).

Received for publication 6 February 1984 and in final form 11 April 1984.

## REFERENCES

1. Hagiwara, S., and L. Byerly. 1981. Calcium channels. *Annu. Rev. Neurosci.* 4:69–125.
2. Lux, H. D. 1983. Observations on single Ca channel: an overview. In *Single-channel Recording*. B. Sakmann and E. Neher, editors. Plenum Publishing Corp., New York. 437–449.
3. Reuter, H. 1983. Ca channel modulation by neurotransmitters, enzymes, and drugs. *Nature (Lond.)*. 301:569–574.
4. Fenwick, E. M., A. Marty, and E. Neher. 1982. Sodium and calcium channels in bovine chromaffin cells. *J. Physiol. (Lond.)*. 331:599–635.
5. Kostyuk, P. G., N. S. Veselovsky, and A. Y. Tsyndrenko. 1981. Ionic currents in the somatic membrane of rat dorsal root ganglion neurons. I. Sodium currents. *Neuroscience*. 6:2423–2430.
6. Llinas, R., and Y. Yarom. 1981. Properties and distribution of ionic conductances generating electroresponsiveness of mammalian inferior olivary neurons in vitro. *J. Physiol. (Lond.)*. 315:569–584.
7. Dunlap, K., and G. Fischbach. 1981. Neurotransmitters decrease the calcium conductance activated by depolarization of embryonic chick sensory neurones. *J. Physiol. (Lond.)*. 317:519–535.
8. Barde, Y. A., D. Edgar, and H. Thoenen. 1980. Sensory neurons in culture: changing requirements for survival factors during embryonic development. *Proc. Natl. Acad. Sci. USA*. 77:1199–1203.
9. Hamill, O. P., A. Marty, E. Neher, B. Sakmann, and E. F. J. Sigworth. 1981. Improved patch-clamp techniques for high-resolution current recording from cells and cell-free membrane patches. *Pfluegers Arch. Eur. J. Physiol.* 391:85–100.
10. Lux, H. D., and A. M. Brown. 1984. Patch and whole cell calcium currents recorded simultaneously in snail neurons. *J. Gen. Physiol.* 83:727–750.
11. Marty, A., and E. Neher. 1983. Tight-seal whole cell recording. In *Single Channel Recording*. B. Sakmann and E. Neher, editors. Plenum Publishing Corp., New York. 107–122.
12. Hodgkin, A., and A. F. Huxley. 1952. The dual effect of membrane potential on sodium conductance in the giant axon of *Loligo*. *J. Physiol. (Lond.)*. 116:497–506.
13. Chandler, W. K., and H. Meves. 1970. Slow changes in membrane permeability and long lasting action potentials in axons perfused with fluoride solutions. *J. Physiol. (Lond.)*. 211:707–728.
14. Fox, J. M. 1976. Ultra-slow inactivation of the ionic currents through the membrane of the myelinated nerve. *Biochim. Biophys. Acta*. 426:245–257.
15. Kostyuk, P. G., O. A. Krishtal, and Y. A. Shakhvalov. 1977. Separation of sodium and calcium currents in the somatic membrane of mollusc neurones. *J. Physiol. (Lond.)*. 270:545–568.
16. Akaike, N., K. S. Lee, and A. M. Brown. 1978. The calcium current of *Helix* neuron. *J. Gen. Physiol.* 71:509–531.
17. Lee, K. S., and R. W. Tsien. 1982. Reversal of current through

- calcium channels in dialyzed single heart cells. *Nature (Lond.)*. 297:498–501.
18. Brown, A. M., Y. Tsuda, and D. L. Wilson. 1983. A description of activation and conduction in calcium channels based on tail and turn-on current measurements. *J. Physiol. (Lond.)*. 344:549–583.
  19. Marquardt, D. W. 1963. An algorithm for least-square estimation of non-linear parameters. *J. Ind. Appl. Math.* 11:431–441.
  20. Moolenaar, W. H., and I. Spector. 1978. Ionic currents in cultured mouse neuroblastoma cells under voltage-clamp conditions. *J. Physiol. (Lond.)*. 278:265–286.
  21. Sigworth, F. J., and E. Neher. 1980. Single Na<sup>+</sup> channel currents observed in cultured rat muscle cells. *Nature (Lond.)*. 287:447–449.
  22. Llinas, R., and H. Jahnsen. 1982. Electrophysiology of mammalian thalamic neurones in vitro. *Nature (Lond.)*. 297:406–408.
  23. Hagiwara, S., S. Ozawa, and O. Sand. 1975. Voltage clamp analysis of two inward current mechanisms in the egg cell membrane of a starfish. *J. Gen. Physiol.* 65:617–644.
  24. Kameyama, M. 1983. Ionic currents in cultured dorsal root ganglion cells from adult guinea pigs. *J. Membr. Biol.* 72:195–203.
  25. Adams, D. J., and P. W. Gage. 1979. Sodium and calcium gating currents in an *Aplysia* neuron. *J. Physiol. (Lond.)*. 291:467–481.
  26. Carbone, E., and H. D. Lux. 1984. Single Ca channel event observed in cultured chick dorsal root ganglion cells: evidence for two types of channels. *Pfluegers Arch. Eur. J. Physiol.* 400(Suppl):40.
  27. Carbone, E., and H. D. Lux. 1984. A low voltage-activated, fully inactivating calcium channel in vertebrate sensory neurones. *Nature (Lond.)*. In press.